membranes

MDPI

Article

Thermoelectric Behavior of $BaZr_{0.9}Y_{0.1}O_{3-d}$ Proton Conducting Electrolyte

Dmitry Tsvetkov [1,*], Ivan Ivanov [1], Dmitry Malyshkin [1,2], Vladimir Sereda [1,2] and Andrey Zuev [1]

1 Institute of Natural Sciences and Mathematics, Ural Federal University, Ekaterinburg 620000, Russia; Ivan.Ivanov@urfu.ru (I.I.); Dmitry.Malyshkin@urfu.ru (D.M.); Vladimir.Sereda@urfu.ru (V.S.); Andrey.Zuev@urfu.ru (A.Z.)

2 Institute of High Temperature Electrochemistry, Ural Branch of Russian Academy of Sciences, Ekaterinburg 620000, Russia

* Correspondence: Dmitry.Tsvetkov@urfu.ru; Tel.: +73432517927

Received: 13 August 2019; Accepted: 11 September 2019; Published: 19 September 2019

Abstract: $BaZr_{0.9}Y_{0.1}O_{3-\delta}$ (BZY10), a promising proton conducting material, exhibits p-type conduction under oxidative conditions. Holes in BZY10 are of the small polaron type. However, there is no clear understanding at which places in the lattice they are localized. The main objectives of this work were, therefore, to discuss the nature of electronic defects in BZY10 on the basis of the combined measurements of the thermo-EMF and conductivity. Total electrical conductivity and Seebeck coefficient of BZY10 were simultaneously studied depending on partial pressures of oxygen (pO_2), water (pH_2O) and temperature (T). The model equation for total conductivity and Seebeck coefficient derived on the basis of the proposed defect chemical approach was successfully fitted to the experimental data. Transference numbers of all the charge carriers in BZY10 were calculated. The heat of transport of oxide ions was found to be about one half the activation energy of their mobility, while that of protons was almost equal to the activation energy of their mobility. The results of the Seebeck coefficient modeling indicate that cation impurities, rather than oxygen sites, should be considered as a place of hole localization.

Keywords: proton conductor; $BaZr_{0.9}Y_{0.1}O_{2.95}$; seebeck coefficient; conductivity; hydration

1. Introduction

Perovskite-type yttrium-doped barium zirconate $BaZr_{0.9}Y_{0.1}O_{3-\delta}$ (BZY10) is a well-known proton conducting material promising for intermediate-temperature electrochemical applications due to high proton conductivity and good chemical stability [1–4]. The defect chemistry of BZY10, which is of key importance for understanding its conductivity, was studied using a number of techniques such as thermogravimetry (TGA) in water vapour containing atmosphere [2,3,5,6], conductivity measurements under wide range of conditions [4,5,7], quasi-elastic neutron scattering (QENS) [8,9], nuclear magnetic resonance (NMR) [10], X-ray absorption spectroscopy (XAS) [11] and computer simulations [12–15]. As a result, the nature of proton defects in BZY10 is relatively well studied [16,17]. However, this is definitely not the case concerning electronic defects. Indeed, it is well known that under certain conditions BZY10 exhibits significant hole-type electronic conductivity comparable to, or even exceeding, the ionic one [5–7]. This p-type conductivity arises due to the partial filling of oxygen vacancies, created through Y-doping, by oxygen under an oxidizing atmosphere [18–20]. In our previous paper [21] we showed that holes in BZY10 are of the small polaron type and exhibit rather strong trapping by some acceptor impurity. Besides yttrium dopant cations, various 3d-metal cations, small amounts of which are always present in any material and are sometimes intentionally

introduced during the synthesis as sintering aids [22–24], may act as a hole trap. So far, however, it is not clear on which positions in the lattice that the non-trapped holes are localized. The assumption that the holes are associated with the oxygen sites is consistent with the results of BZY10 electronic structure calculations [25] and in line with the conclusions of Schirmer and others [26] and references therein, in regards to the nature of holes in the great number of different oxide materials. However, the hypothesis that the holes are localized on the impurity ions is also quite plausible, taking into account the rather small concentration of holes present in BZY10. In this respect, it is worth noting that the thermoelectric behaviour of $BaZr_{1-x}Y_xO_{3-d}$ proton conducting oxides has not been studied and discussed in detail so far, contrary to electrical conductivity, although thermoelectric power measurements were shown to provide valuable data necessary for elucidating the nature of defects and charge transfer in case of the state-of-the-art oxide ion conductors and mixed conductors [27–34]. Therefore, combining the thermo-EMF and conductivity measurements should advance the understanding of both defect chemistry and charge transfer in proton conductors.

Therefore, the main objectives of this work are (i) to study the thermoelectric behaviour of proton conducting oxide BZY10 and its electrical conductivity in the wide range of temperatures (T), oxygen (pO_2) and water vapour (pH_2O) partial pressures, and (ii) to discuss the nature of electronic defects in BZY10 in the light of these measurements.

2. Materials and Methods

The powder sample of BZY10 was prepared by means of glycerol-nitrate method described elsewhere [15]. High-purity $BaCO_3$ (99.99%, Lanhit, Moscow, Russia), $Zr(OH)_2CO_3$ (99.9%, ChMZ, Glazov, Russia) and Y_2O_3 (99.99%, Lanhit, Moscow, Russia) were used as starting materials. The BZY10 powder was calcined three times at 1100 °C in air. As-prepared powder was pressed at 154–160 MPa into tablets 20 mm in diameter and then sintered at 1500 °C for 24 h in air with 100 °C/h as a heating/cooling rate. Before the sintering procedure, green tablets were covered by the sacrificial powder of the same chemical composition in order to prevent Ba loss due to volatility of its oxide at high temperatures. The relatively moderate sintering temperature was chosen because of the same reason. Rectangular bars of $20 \times 3 \times 3$ mm^3 for the conductivity and Seebeck coefficient measurements were cut from the tablets sintered accordingly. The as-obtained bars had 85–90% relative density. The residual porosity promoted sample equilibration with the gas phase, as discussed in detail by Wang and Virkar [16]. This significantly reduced the time necessary for the sample equilibration and, consequently, allowed for obtaining reproducible equilibrium values of all the properties studied in this work.

The phase composition of the sample prepared accordingly was studied by means of X-ray diffraction (XRD) using an XRD 7000 diffractometer (Shimadzu, Kyoto, Japan). The XRD (Cu Kα radiation) showed no indication for the presence of a second phase in the as-prepared powder of BZY10.

Electrical conductivity was measured by a 4-probe dc method using an original homemade setup [21] equipped with an yttria-stabilized zirconia (YSZ) electrochemical oxygen pump and sensor. The Seebeck coefficient was measured simultaneously in the same setup by placing the sample in the moderate temperature gradient, around 10–15 °C. The uncertainties in the total conductivity and the Seebeck coefficient did not exceed ±5% and ±10 μV/K, respectively. The measurements were carried out depending on T, pO_2 and pH_2O.

Water uptake of as-prepared BZY10 was measured by the thermogravimetric technique (TG) [35]. The measurements were carried out in the temperature range 25–900 °C in the atmosphere of air ($\log(pO_2/\text{atm}) = -0.677$) or nitrogen ($\log(pO_2/\text{atm}) = -4.5$) and in the range of water vapor partial pressure ($-1.73 \leq \log(pH_2O/\text{atm}) \leq -4.0$).

The atmosphere employed in the thermo-EMF, conductivity and TG measurements was dried by circulating the gas through the column filled with pre-annealed zeolites. The residual water vapor pressure was found to be $\log(pH_2O/\text{atm}) = -4.0$. The humidity of the gas (i.e., pH_2O) was measured using the original unit on the basis of the H_2O-sensor BME-280 (Bosch, Stuttgard, Germany).

3. Results and Discussion

The XRD pattern of the as-prepared single-phase BZY10 was indexed using the cubic $Pm\bar{3}m$ space group and is shown in Figure 1 along with the Rietveld refinement results. The refined value of BZY10 lattice parameter, a = (4.2075 ± 0.0001) Å, is in good agreement with its values reported previously [1–5,7].

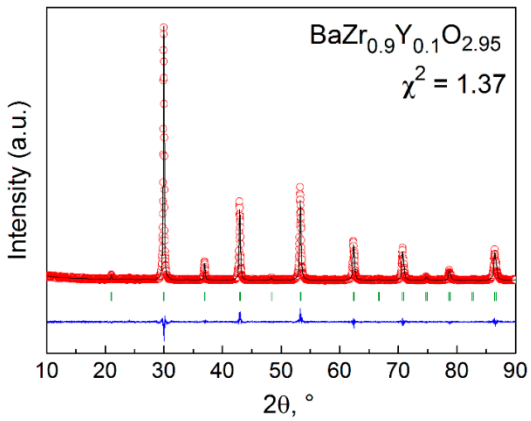

Figure 1. Rietveld refined XRD pattern of BZY10 sample slowly (~100 °C/h) cooled from 1500 °C to room temperature in dry air (log(pH$_2$O/atm) = −4.0): Observed X-ray diffraction intensity (points) and calculated curve (line). The bottom curve is the difference of patterns, y_{obs}-y_{cal}, and the small bars indicate the angular positions of the allowed Bragg reflections

The total conductivity and Seebeck coefficient of BZY10 were measured as a function of pO$_2$, pH$_2$O and T in the ranges −18 ≤ log(pO$_2$ /atm) ≤ −0.67, −4 ≤ log(pH$_2$O /atm) ≤ −1.73 and 688 ≤ T (°C) ≤ 1038. As an example, the results obtained at log(pH$_2$O /atm) = −1.73 are shown in Figure 2.

Table 1. Fitted parameters of Equation (4)

Charge Carrier	Pre-Exponential Factor [1], S·cm^{-1}	Activation Energy [1], eV	R^2
Oxide ion	25.43 ± 13.00	1.42 ± 0.01	
Hole	10.42 ± 3.00	0.73 ± 0.05	0.997
Proton	(1.47 ± 0.60)·10^{-3}	0.02 ± 0.09	

[1] Uncertainties are given as two standard deviations as obtained by fitting procedure.

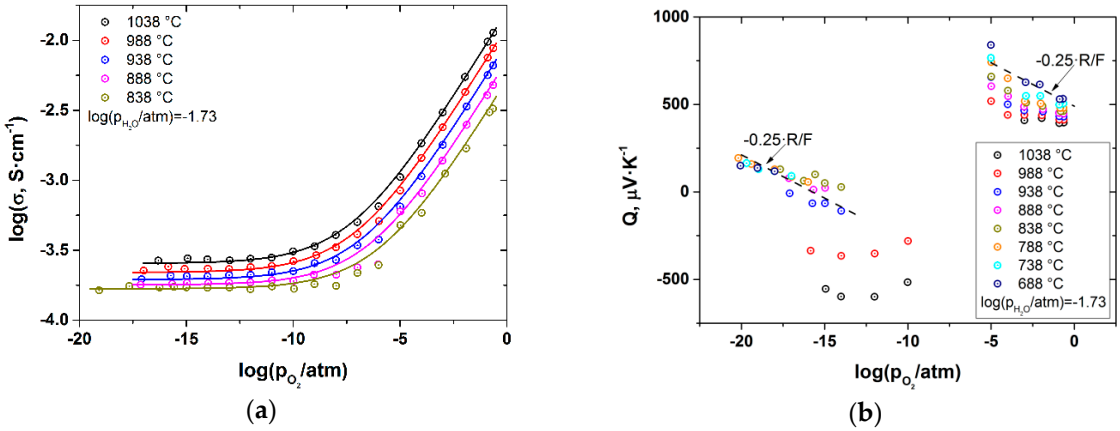

Figure 2. Total conductivity (**a**) and Seebeck coefficient (**b**) of BZY10 measured at log(pH$_2$O/atm) = −1.73 as a function of T and pO$_2$. Points-experimental results, solid lines-calculation according to Equation (4) with parameters given in Table 1.

As seen, the total conductivity behavior is typical of many proton-conducting oxides, with a characteristic slope of 1/4 corresponding to a p-type contribution under oxidizing conditions and almost pO_2-independent ionic part. The ionic contribution was found to possess the pH_2O dependence with a characteristic slope of 1/2 under reducing atmosphere. At the same time, the Seebeck coefficient is positive and grows with decreasing pO_2 under oxidizing atmosphere. Under reducing conditions ($pO_2 < 10^{-5}$), it drops abruptly, becoming negative, and increases upon subsequent pO_2 decrease. It is also to be emphasized that within the pO_2 range of 10^{-10}–10^{-5} atm it was impossible to obtain stable values of Seebeck coefficient. The reason for both the abrupt change and the instability of Seebeck coefficient mentioned above is most probably related to the fact that the heterogeneous part of the thermo-EMF is strongly dependent on the chemical potential of oxygen in the surrounding atmosphere [27,31,33,34]. The chemical potential, in turn, is determined by gaseous O_2 under oxidizing conditions ($10^{-5} \le pO_2 \le 0.21$ atm) and by the H_2/H_2O chemical equilibrium under reducing atmosphere (at pO_2 lower then ~10^{-10} atm). Thus, it is difficult to achieve stable and well-defined chemical potential of oxygen in the intermediate pO_2 range and, consequently, it is also practically impossible to get reliable values of the Seebeck coefficient. Therefore, in order to analyze the behaviour of sample's thermoelectric power and to see its overall trend vs. pO_2, one needs to normalize the Seebeck coefficient measured in H_2/H_2O atmosphere against that obtained under the O_2/N_2 atmosphere. It can be easily shown [27,31,33,34] that the difference between the coefficients measured at the same pO_2 under O_2/N_2 atmosphere, Q_1, and in the H_2/H_2O gas mixture, Q_2, is equal to:

$$Q_1 - Q_2 = -\frac{t_O + t_H}{2F}\frac{\Delta_f H^\circ_{H_2O}}{T} \quad (1)$$

where t_O and t_H, $\Delta_f H^\circ_{H_2O}$ and F are transference number of oxide ions and protons, and standard formation enthalpy of gaseous water and Faraday constant, respectively. Therefore, transference numbers of ionic species in BZY10 are required to perform this normalization procedure. In order to calculate them it is necessary to separate contributions of all the charge carriers (their partial conductivities) to the total conductivity of BZY10. At relatively high temperatures, employed in this work, holes and protons are minority defects and, therefore, the charge neutrality condition for BZY10 can be written as $\left[Y'_{Zr}\right] = 2\left[V^{\bullet\bullet}_O\right]$. As a result, concentrations of holes and protons can be expressed as [21]:

$$p = K \cdot p_{O_2}^{1/4}, \left[OH^\bullet_O\right] = K' \cdot p_{H_2O}^{1/2} \quad (2)$$

where K and K' are proportionality constants which can be related to the equilibrium constants corresponding to the defect reactions describing the formation of the charge carriers, as discussed in [21]. Since holes were shown in our previous work [21] to exhibit strong trapping by acceptor impurities, most probably by the dopant, Y'_{Zr}, therefore, p in the Equation (2) denotes the concentration of 'free', non-trapped small polaron holes. These considerations finally result in the following equation for the total conductivity:

$$\sigma = \sigma_O + \sigma^\circ_p \cdot p_{O_2}^{1/4} + \sigma^\circ_H \cdot p_{H_2O}^{1/2} \quad (3)$$

where σ_O, σ°_p and σ°_H are oxide ion conductivity, hole conductivity at pO_2 = 1 atm and proton conductivity at pH_2O=1 atm, respectively. Each of these conductivities, in turn, is thermally activated and, as a consequence, can be represented using Arrhenius-type equation. This leads to the Equation (4) which can be fitted to the experimental data on total conductivity of BZY10:

$$\sigma = A \cdot \exp\left(-\frac{E_{A,O}}{RT}\right) + B \cdot \exp\left(-\frac{E_{A,p}}{RT}\right) \cdot p_{O_2}^{1/4} + C \cdot \exp\left(-\frac{E_{A,H}}{RT}\right) \cdot p_{H_2O}^{1/2} \quad (4)$$

where A, B and C are corresponding pre-exponential factors and $E_{A,O}$, $E_{A,p}$ and $E_{A,H}$ are activation energies of oxide ion, hole and proton conduction, respectively. A 4D-fitting procedure was used since total conductivity depends on three independent parameters—T, pO_2 and pH_2O, as follows

from Equation (4). This allowed fitting all the data on total conductivity of BZY10 simultaneously. The fitting results are summarized in Table 1 and, as an example, are shown in Figure 3 as 3D-plots at two temperatures −1038 and 838 °C, and in Figure 2 as a 2D-plot at $\log(pH_2O/atm) = -1.73$.

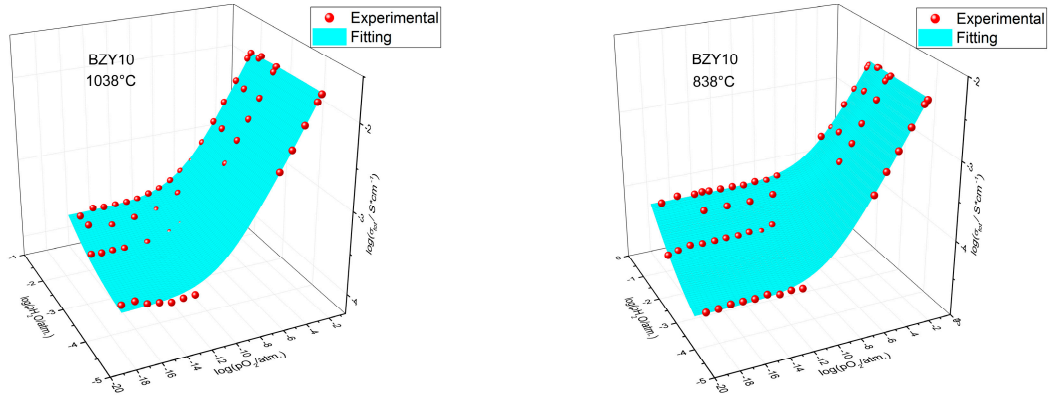

(**a**) (**b**)

Figure 3. The results of fitting for BZY10 total conductivity at (**a**) 1038 °C and (**b**) 838 °C. Points-experimental data, surface-results of calculation according to Equation (4) with fitted parameters given in Table 1.

Interestingly, the activation energy of proton conduction was fitted as equal to zero within the uncertainty limits, as seen in Table 2. The reason for this is, obviously, two counteracting trends: The increase in thermally activated mobility of protons with temperature and simultaneous decrease in their concentration due to dehydration (see Appendix A). The activation energy of proton mobility in BZY10 was reported to be about 0.44 eV [2,3,36]. Combining this value with the activation energy given in Table 1 allows estimating the hydration enthalpy as about −0.84 eV or −81 kJ·mol^{-1}, which is in excellent agreement with values reported in literature [2,3,5,37] and determined by us from the TGA results (see Appendix A). The parameters given in Table 1 allow calculation of partial conductivities and transference numbers of all charge carriers in BZY10. Examples of such calculations are shown in Figure 4 where transference numbers are presented as a function of pO_2 and pH_2O at 1038 °C.

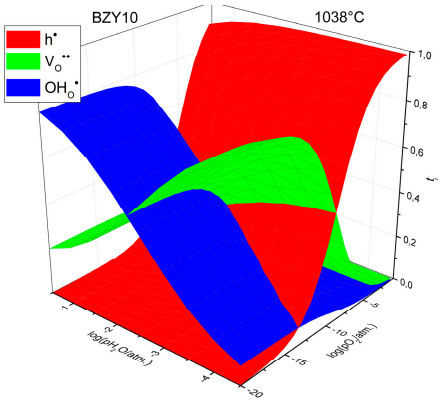

Figure 4. Transference numbers of charge carriers in BZY10 depending on pO_2 and pH_2O at 1038 °C.

As seen, BZY10 is mainly ionic conductor (with dominating proton conductivity under wet atmosphere and oxide ion conductivity under dry atmosphere) at elevated temperatures under reducing conditions, whereas the hole conductivity dominates under oxidizing conditions. This conclusion is in agreement with similar observations of others [5–7].

Using the calculated transference numbers, it is possible to perform the normalization procedure described above for Seebeck coefficient. Thermodynamic data necessary for calculation according to

Equation (1) were taken from [38]. The as-normalized Seebeck coefficient is shown in Figure 5 as a function of pO_2 at different temperatures and at $\log(pH_2O/atm) = -1.73$.

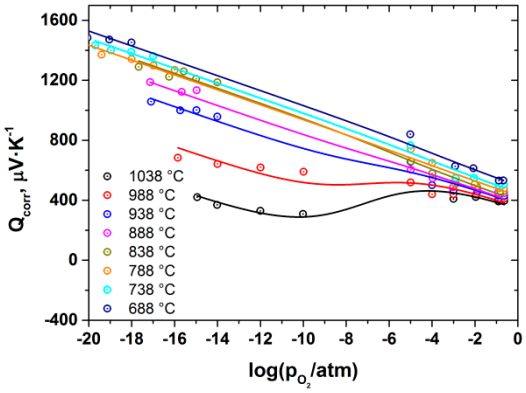

Figure 5. Normalized Seebeck coefficient of BZY10 vs. pO_2 at $\log(pH_2O/atm) = -1.73$. Points-experimental data, lines-result of the fit of Equation (5).

Normalized Seebeck coefficient of the proton conductor can be represented [39] as:

$$Q = t_p\theta_p + t_O\theta_O + t_H\theta_H + \frac{t_O + t_H}{4F}\left(S^\circ_{O_2} - R\ln p_{O_2}\right) + \frac{t_H}{2F}\left(-S^\circ_{H_2O} + R\ln p_{H_2O}\right) \quad (5)$$

where θ_p, θ_O and θ_H are partial Seebeck coefficients of holes, oxide ions and protons, respectively. These partial contributions may be defined by the following equation [27,39]:

$$\theta_i = \frac{1}{z_i F}\left(\overline{s_i} + \frac{q_i^*}{T}\right) \quad (6)$$

where $\overline{s_i}$ is partial molar entropy of charge carrier and q_i^*—its heat of transport. The calculation of $\overline{s_i}$ allows obtaining the following expressions for partial Seebeck coefficients [27,31,39,40]:

$$\theta_p = \frac{R}{F}\left(\ln\frac{N-p}{p} + \frac{q_p^*}{RT}\right) \quad (7)$$

$$\theta_O = -\frac{R}{2F}\left(\frac{\overline{s}_{O(vibr)}}{R} + \ln\frac{\left[V_O^{\bullet\bullet}\right]}{3 - \left[V_O^{\bullet\bullet}\right] - \left[OH_O^{\bullet}\right]} + \frac{q_H^*}{RT}\right) \quad (8)$$

$$\theta_H = \frac{R}{F}\left(\frac{\overline{s}_{H(vibr)}}{R} + \ln\frac{3 - \left[V_O^{\bullet\bullet}\right] - \left[OH_O^{\bullet}\right]}{\left[OH_O^{\bullet}\right]} + \frac{q_O^*}{RT}\right) \quad (9)$$

where N is a number of positions available for holes, $\overline{s}_{O(vibr)}$ and $\overline{s}_{H(vibr)}$ are vibrational contributions to the entropy of oxide ions and protons, respectively. According to Tsidilkovsky et al. [39,40], vibrational contribution to the chemical potential of an ionic species (oxide ions or protons) can be estimated in the harmonic approximation as follows:

$$\Delta\mu_{i,(vibr)} = RT\sum_{i=1}^{3}\ln\left(2\sinh\left[\frac{\hbar\omega_i}{2kT}\right]\right) \quad (10)$$

where ω_i—vibration frequency of proton or oxide ion. In this model, the following set of three frequencies is used for both protons and oxide ions: $\omega_H\left(cm^{-1}\right) = \{3400,\ 960,\ 960\}$ and $\omega_O\left(cm^{-1}\right) =$

{550, 250, 250}, respectively [39,40]. The vibrational contribution to the entropy of ionic charge carriers can then be calculated as follows:

$$\Delta\bar{s}_{i,(vibr)} = -\left(\frac{\partial\Delta\mu_{i,(vibr)}}{\partial T}\right) = -R\sum_{i=1}^{3}\ln\left(2\sinh\left[\frac{\hbar\omega_i}{2kT}\right]\right) + RT\sum_{i=1}^{3}\frac{\hbar\omega_i\cosh\left[\frac{\hbar\omega_i}{2kT}\right]}{2kT^2} \quad (11)$$

Equations (7)–(11) were substituted into Equation (5). The concentration of holes was taken as $p = \exp\left(\frac{\Delta S_p^\circ}{R} - \frac{\Delta H_p^\circ}{RT}\right)p_{O_2}^{1/4}$, where ΔS_p° and ΔH_p° are standard entropy and enthalpy of hole formation, respectively. The concentration of protons was calculated from the results of the separate TGA experiment (see Appendix A). Finally, when all the necessary terms were substituted to Equation (5), the Seebeck coefficient was expressed as a function $Q = f\left(T,\ pO_2,\ q_p^*,\ q_O^*,\ q_H^*,\ \Delta S_p^\circ,\ \Delta H_p^\circ,\ N\right)$. The unknown parameters: q_p^*, q_O^*, q_H^*, ΔS_p° and ΔH_p° were determined by fitting Equation (5) to the data on normalized Seebeck coefficient vs. T and pO_2 at fixed log (pH_2O/atm) = –1.73, i.e., a 3D-fitting procedure was employed and all the data were treated simultaneously. The results of the fit are summarized in Table 2 and shown in Figure 5 as 3D- and 2D-plots. It is to be noted that strong correlation between the values of ΔS_p° and q_p^* was found during the fitting procedure, therefore, q_p^* was set equal to zero which seems to be the common assumption in the case of small polarons [28–30].

Table 2. Fitted parameters of Equation (5).

Charge Carrier	Heat of Transport, eV *	ΔS_p°, J·mol^{-1}·K^{-1}*	ΔH_p°, kJ·mol^{-1}*	R^2
Oxide ion	0.73 ± 0.03	34.6 ± 1.4 (N = 2.95)	0.74 ± 0.04 (does not depend on N)	0.990
Hole	0 **	6.5 ± 1.4 (N = 0.1)		
Proton	0.43 ± 0.10	−12.3 ± 1.4 (N = 0.01)		

* Uncertainties are given as two standard deviations as obtained by fitting procedure. ** q_p^* was arbitrarily set equal to zero (please, see the explanation in the text)

Furthermore, parameters N and $K = \exp\left(\frac{\Delta S_p^\circ}{R} - \frac{\Delta H_p^\circ}{RT}\right)$ are also strongly interdependent, since both of them enter in the same part of Equation (7): N—in the numerator and K—both in the numerator and denominator. As seen in Table 2, fitting leads to different values of ΔS_p° parameter depending on the particular value of N selected. At the same time, the enthalpy ΔH_p° obtained during the fitting procedure is always the same irrespective of a value of N. Therefore, additional assumptions on the particular value of N are needed in order to evaluate K and then to estimate the concentration of non-trapped holes according to Equation (2). This calculation sequence allows for some speculation on the possible sites available for holes. Indeed, both the charge neutrality condition employed, $\left[Y_{Zr}^{/}\right] = 2\left[V_O^{\bullet\bullet}\right]$, and excellent quality of fit of Equation (4) to the total conductivity data of BZY10 may imply that holes, either trapped or 'free', are minority charge carriers, i.e., that their concentration is expected to be very small. At the same time, fitting Equation (5) under assumption that $N = \left[O_O^{\times}\right] = 2.95$, which means that holes are associated with oxygen sites, leads to a large positive value of ΔS_p° parameter (see Table 2) and, in combination with $\Delta H_p^\circ = 0.74$ eV, to abnormally large value of constant K: for example, K = 0.092 at 1038 °C. This results in extraordinarily large concentration of non-trapped holes, e.g., p = 0.062 at pO_2 = 0.21 atm. A much better agreement with physical meaning is obtained when setting lower values of N, for example, at N = 0.1 one can obtain $K = 3.12 \times 10^{-3}$ and p = 0.0021 at 1038 °C and pO_2 = 0.21 atm. It may well be that an even significantly lower value of N is not unreasonable. Therefore, these simple calculations do not indicate in favor of oxygen sites as a place for localization of holes, contrary to the common belief [25,26,41–46]. It seems more likely that the holes are localized on the cation impurities, especially taking into account that significantly different conductivity values were reported for BZY10 by different authors [7,47]. Indeed, different acceptor impurity concentrations may be responsible for such scatter in the reported conductivity values. In order to understand the nature of holes in more detail, it would be of interest to prepare a number of samples with a controlled

amount of some selected impurities and then measure and compare their properties. This work is in progress now.

It is also worth mentioning that for the oxide ions the heat of transport is about one half their activation energy of mobility (see Table 1), whereas for the protons these values are almost the same.

4. Conclusions

The sample of BZY10 proton conducting electrolyte was prepared and its electrical conductivity and Seebeck coefficient were studied in the wide range of conditions. Conductivity as a function of pO_2, pH_2O and T was successfully fitted by the model equation derived on the basis of the defect chemical approach. The fitted model parameters allowed calculation of the transference numbers of all the charge carriers involved. The Seebeck coefficient of BZY10, measured under a reducing atmosphere, was normalized to that measured under oxidative conditions in order to account for the shift in heterogeneous part of thermo-EMF when going from N_2/O_2 to H_2/H_2O gas mixture. Normalized Seebeck coefficient of BZY10 as a function of pO_2, pH_2O and T was fitted by the appropriate model equation containing the weighted sum of partial Seebeck coefficients of each charge carrier and heterogeneous part that depends on the chemical potential of oxygen and water vapor. The heats of transport of oxide ions and protons were found to be about one half of the activation energy of mobility and almost equal to that, respectively. Fitting results of the Seebeck coefficients also revealed that oxygen sites do not seem to be responsible for the formation of small polaron holes, rather, some cation impurities should be considered.

Author Contributions: Conceptualization and methodology, D.T. and I.I.; investigation, I.I., D.M. and V.S.; writing-original draft preparation, D.T. and A.Z.; supervision, A.Z.

Funding: This work was supported by the Russian Science Foundation (project No. 18-73-00022).

Conflicts of Interest: The authors declare no conflicts of interest. The funders had no role in the design of the study; in the collection, analyses, or interpretation of data; in the writing of the manuscript, or in the decision to publish the results.

Appendix A

Hydration of the BZY10 sample was studied by TG. The as-measured water content in the sample is shown in Figure A1 at $\log(pH_2O/\text{atm}) = -1.76$ as a function of temperature.

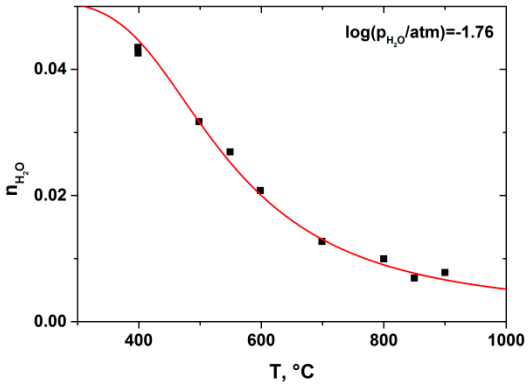

Figure A1. Water uptake of BZY10 vs. T at $\log(pH_2O/\text{atm}) = -1.76$. Points-experimental data, line-result of the fit of Equation (A3).

Hydration of BZY10 can be described using the following quasichemical reaction [2,3] written using Kröger-Vink notation:

$$H_2O + V_O^{\bullet\bullet} + O_O^{\times} \rightleftarrows 2OH_O^{\bullet} \quad \text{(A1)}$$

with equilibrium constant

$$K_{hydr} = \exp\left(\frac{\Delta S^{\circ}_{hydr}}{R} - \frac{\Delta H^{\circ}_{hydr}}{RT}\right) = \frac{\left[OH^{\bullet}_{O}\right]^2}{p_{H_2O}\left[V^{\bullet\bullet}_{O}\right]\left[O^{\times}_{O}\right]} \quad \text{(A2)}$$

where ΔS°_{hydr} and ΔH°_{hydr} are standard entropy and enthalpy of BZY10 hydration, respectively. Taking into account charge balance and mass balance conditions [2,3] the following solution of the Equation (A2) can be obtained:

$$\left[OH^{\bullet}_{O}\right] = 2n_{H_2O} = -\frac{2.95}{4}K_{hydr}p_{H_2O} + \frac{1}{4}\sqrt{8.7025 \cdot K^2_{hydr}p^2_{H_2O} + 2.36 \cdot K_{hydr}p_{H_2O}} \quad \text{(A3)}$$

Equation (A3) was fitted to the experimental data on the water uptake of BZY10 in order to determine ΔS°_{hydr} and ΔH°_{hydr}. The results of the fit are summarized in Table A1 and shown in Figure A1. Equation (A3) with fitted ΔS°_{hydr} and ΔH°_{hydr} was used to calculate concentration of protons in BZY10 in order to estimate partial ionic Seebeck coefficients of protons and oxide ions according to Equations (8) and (9).

Table A1. Fitted parameters of Equation (A3).

ΔH°_{hydr}, kJ·mol^{-1}*	ΔS°_{hydr}, J·mol−^{1}K^{-1}*	R^2
−79 ± 2	−91 ± 2	0.992

* Uncertainties are given as two standard deviations as obtained by fitting procedure.

References

1. Sažinas, R.; Einarsrud, M.-A.; Grande, T. Toughening of Y-doped $BaZrO_3$ proton conducting electrolytes by hydration. *J. Mater Chem. A* **2017**, *5*, 5846–5857. [CrossRef]
2. Kreuer, K.D. Aspects of the formation and mobility of protonic charge carriers and the stability of perovskite-type oxides. *Solid State Ionics* **1999**, *125*, 285–302. [CrossRef]
3. Kreuer, K.D. Proton-conducting oxides. *Annu. Rev. Mater. Res.* **2003**, *33*, 333–359. [CrossRef]
4. Medvedev, D.; Brouzgou, A.; Demin, A.; Tsiakaras, P. *Advances in Medium and High Temperature Solid Oxide Fuel Cell Technology*; Boaro, M., Salvatore, A.A., Eds.; Springer International Publishing: Cham, Switzerland, 2017; pp. 77–118.
5. Schober, T.; Bohn, H.G. Water vapor solubility and electrochemical characterization of the high temperature proton conductor $BaZr_{0.9}Y_{0.1}O_{2.95}$. *Solid State Ionics* **2000**, *127*, 351–360. [CrossRef]
6. Ji, H.; Kim, B.; Yu, J.H.; Choi, S.; Kim, H.; Son, J.; Lee, H.; Lee, J. Three dimensional representations of partial ionic and electronic conductivity based on defect structure analysis of $BaZr_{0.85}Y_{0.15}O_{3-\delta}$. *Solid State Ionics* **2011**, *203*, 9–17. [CrossRef]
7. Gorelov, V.P.; Balakireva, V.B. Synthesis and properties of high-density protonic solid electrolyte $BaZr_{0.9}Y_{0.1}O_{3-\alpha}$. *Russ. J. Electrochem.* **2009**, *45*, 476–482. [CrossRef]
8. Karlsson, M. Proton dynamics in oxides: Insight into the mechanics of proton conduction from quasielastic neutron scattering. *Phys. Chem. Chem. Phys.* **2015**, *17*, 26–38. [CrossRef] [PubMed]
9. Noferini, D.; Koza, M.M.; Karlsson, M. Localized proton motions in acceptor-doped barium zirconates. *J. Phys. Chem. C* **2017**, *121*, 7088–7093. [CrossRef]
10. Yamazaki, Y.; Blanc, F.; Okuyama, Y.; Buannic, L.; Lucio-Vega, J.C.; Grey, C.P.; Haile, S.M. Proton trapping in yttrium-doped barium zirconate. *Nat. Mater* **2013**, *12*, 647–651. [CrossRef]
11. Higuchi, T.; Iguchi, F.; Nagao, Y.; Sata, N.; Liu, Y.-S.; Glans, P.-A.; Guo, J.; Yugami, H. Surface Electronic Structure of $BaZr_{1-x}Y_xO_{3-\delta}$ by Soft-X-Ray Spectroscopy. *Trans. Mater Res. Soc. Japan* **2012**, *37*, 575–578. [CrossRef]
12. Björketun, M.E.; Sundell, P.G.; Wahnström, G. Structure and thermodynamic stability of hydrogen interstitials in $BaZrO_3$ perovskite oxide from density functional calculations. *Faraday Discuss.* **2007**, *134*, 247–265. [CrossRef] [PubMed]

13. Sundell, P.G.; Björketun, M.E.; Wahnström, G. Density-functional calculations of prefactors and activation energies for H diffusion in $BaZrO_3$. *Phys. Rev. B* **2007**, *76*, 094301. [CrossRef]
14. Raiteri, P.; Gale, J.D.; Bussi, G. Reactive force field simulation of proton diffusion in $BaZrO_3$ using an empirical valence bond approach. *J. Phys. Cond. Mater* **2011**, *23*, 334213. [CrossRef] [PubMed]
15. Kitamura, N.; Akola, J.; Kohara, S.; Fujimoto, K.; Idemoto, Y. Proton Distribution and Dynamics in Y- and Zn-Doped $BaZrO_3$. *J. Phys. Chem. C* **2014**, *118*, 18846–18852. [CrossRef]
16. Haro-González, P.; Karlsson, M.; Gaita, S.M.; Knee, C.S.; Bettinelli, M. Eu^{3+} as a luminescent probe for the local structure of trivalent dopant ions in barium zirconate-based proton conductors. *Solid State Ionics* **2013**, *247*, 94–97. [CrossRef]
17. Noferini, D.; Koza, M.M.; Rahman, S.M.H.; Evenson, Z.; Nilsen, G.J.; Eriksson, S.; Wildes, A.R.; Karlsson, M. Role of the doping level in localized proton motions in acceptor-doped barium zirconate proton conductors. *Phys. Chem. Chem. Phys.* **2018**, *20*, 13697–13704. [CrossRef] [PubMed]
18. Yamazaki, Y.; Yang, C.-K.; Haile, S.M. Unraveling the defect chemistry and proton uptake of yttrium-doped barium zirconate. *Scripta Mater* **2011**, *65*, 102–107. [CrossRef]
19. Wang, W.; Virkar, A.V. Ionic and electron–hole conduction in $BaZr_{0.93}Y_{0.07}O_{3-\delta}$ by 4-probe dc measurements. *J. Power Sources.* **2005**, *142*, 1–9. [CrossRef]
20. Yamazaki, Y.; Babilo, P.; Haile, S.M. Defect chemistry of yttrium-doped barium zirconate. *Chem. Mater* **2008**, *20*, 6352–6357. [CrossRef]
21. Tsvetkov, D.S.; Ivanov, I.L.; Malyshkin, D.A.; Sereda, V.V.; Zuev, A.Y. Red-Ox energetics and holes trapping in yttrium-substituted barium zirconate $BaZr_{0.9}Y_{0.1}O_{2.95}$. *J. Electrochem. Soc.* **2019**, *166*, F232–F238. [CrossRef]
22. Babilo, P.; Haile, S.M. Enhanced sintering of yttrium-doped barium zirconate by addition of ZnO. *J. Am. Ceram. Soc.* **2005**, *88*, 2362–2368. [CrossRef]
23. Tong, J.; Clark, D.; Bernau, L.; Sanders, M.; O'Hayre, R. Solid-state reactive sintering mechanism for large-grained yttrium-doped barium zirconate proton conducting ceramics. *J. Mater. Chem.* **2010**, *20*, 6333–6341. [CrossRef]
24. Nikodemski, S.; Tong, J.; O'Hayre, R. Solid-state reactive sintering mechanism for proton conducting ceramics. *Solid State Ionics* **2013**, *253*, 201–210. [CrossRef]
25. Lindman, A.; Erhart, P.; Wahnström, G. Polaronic contributions to oxidation and hole conductivity in acceptor-doped $BaZrO_3$. *Phys. Rev. B* **2016**, *94*, 075204. [CrossRef]
26. Schirmer, O.F. O^- bound small polarons in oxide materials. *J. Phys. Cond. Mater* **2006**, *18*, R667–R704. [CrossRef]
27. Wagner, C. The thermoelectric power of cells with ionic compounds involving ionic and electronic conduction. *Prog. Solid State Chem.* **1972**, *7*, 1–37. [CrossRef]
28. Tai, L.-W.; Nasrallah, M.M.; Anderson, H.U.; Sparlin, D.M.; Sehlin, S.R. Structure and electrical properties of $La_{1-x}Sr_xCo_{1-y}Fe_yO_3$. Part 1. The system $La_{0.8}Sr_{0.2}Co_{1-y}Fe_yO_3$. *Solid State Ionics* **1995**, *76*, 259–271. [CrossRef]
29. Tai, L.-W.; Nasrallah, M.M.; Anderson, H.U.; Sparlin, D.M.; Sehlin, S.R. Structure and electrical properties of $La_{1-x}Sr_xCo_{1-y}Fe_yO_3$. Part 2. The system $La_{1-x}Sr_xCo_{0.2}Fe_{0.8}O_3$. *Solid State Ionics* **1995**, *76*, 273–283. [CrossRef]
30. Sehlin, S.R.; Anderson, H.U.; Sparlin, D.M. Semiempirical model for the electrical properties of $La_{1-x}Ca_xCoO_3$. *Phys. Rev. B.* **1995**, *52*, 11681–11689. [CrossRef] [PubMed]
31. Yamaguchi, S.; Kobayashi, K.; Abe, K.; Yamazaki, S.; Iguchi, Y. Electrical conductivity and thermoelectric power measurements of $Y_2Ti_2O_7$. *Solid State Ionics* **1998**, *113–115*, 393–402. [CrossRef]
32. Koshibae, W.; Tsutsui, K.; Maekawa, S. Thermopower in cobalt oxides. *Phys. Rev. B.* **2000**, *62*, 6869–6872. [CrossRef]
33. Park, S.-H.; Yoo, H.-I. Thermoelectric behavior of a mixed ionic electronic conductor, $Ce_{1-x}Gd_xO_{2-x/2-d}$. *Phys. Chem. Chem. Phys.* **2009**, *11*, 391–401. [CrossRef] [PubMed]
34. Ahlgren, E.; Poulsen, F.W. Thermoelectric power of YSZ. *Solid State Ionics* **1994**, *70*, 528–532. [CrossRef]
35. Sereda, V.; Malyshkin, D.; Tsvetkov, D.; Zuev, A. Hydration thermodynamics of proton-conducting perovskite $Ba_4Ca_2Nb_2O_{11}$. *Mater Lett.* **2019**, *235*, 97–100. [CrossRef]
36. Bohn, H.G.; Schober, T. Electrical conductivity of the high-temperature proton conductor $BaZr_{0.9}Y_{0.1}O_{2.95}$. *J. Am. Ceram. Soc.* **2000**, *83*, 768–772. [CrossRef]
37. Kjølseth, C.; Wang, L.-Y.; Haugsrud, R.; Norby, T. Determination of the enthalpy of hydration of oxygen vacancies in Y-doped BaZrO3 and BaCeO3 by TG-DSC Solid State Ionics. *Solid State Ionics* **2010**, *181*, 1740–1745.

38. Gurvich, L.V. *Thermodynamic Properties of Individual Substances*, 4th ed.; Hemisphere Publishing Corp.: New York, NY, USA, 1989.
39. Tsidilkovski, V.I.; Putilov, L.P. The role of deep acceptor levels in hydration and transport processes in $BaZr_{1-x}Y_xO_{3-\delta}$ and related materials. *J. Solid State Electrochem.* **2016**, *20*, 629–643. [CrossRef]
40. Putilov, L.P.; Tsidilkovski, V.I. The role of deep acceptor centers in the oxidation of acceptor-doped wideband-gap perovskites ABO_3. *J. Solid State Chem.* **2017**, *247*, 147–155. [CrossRef]
41. Stokes, S.J.; Islam, M.S. Defect chemistry and proton-dopant association in $BaZrO_3$ and $BaPrO_3$. *J. Mater. Chem.* **2010**, *20*, 6258–6264. [CrossRef]
42. Zhu, H.; Ricote, S.; Coors, W.G.; Kee, R.J. Interpreting equilibrium-conductivity and conductivity-relaxation measurements to establish thermodynamic and transport properties for multiple charged defect conducting ceramics. *Faraday Discuss.* **2015**, *182*, 49–74. [CrossRef]
43. Zhu, H.; Kee, R.J. Membrane polarization in mixed-conducting ceramic fuel cells and electrolyzers. *Int. J. Hydrogen Energy* **2016**, *41*, 2931–2943. [CrossRef]
44. Zhu, H.; Ricote, S.; Duan, C.; O'Hayre, R.P.; Tsvetkov, D.S.; Kee, R.J. Defect incorporation and transport within dense $BaZr_{0.8}Y_{0.2}O_{3-\delta}$ (BZY20) proton-conducting membranes. *J. Electrochem. Soc.* **2018**, *165*, F581–F588. [CrossRef]
45. Ma, F.; Raymond, M.V.; Smyth, D.M. Hole-trapping in $ATiO_3$, (A = Ba, Sr, Ca). *Ferroelectrics* **2006**, *331*, 43–51. [CrossRef]
46. Raymond, M.V.; Smyth, D.M. Defect chemistry and transport properties of $Pb(Zr_{1/2}Ti_{1/2})O_3$. *Integr. Ferroelectr.* **1994**, *4*, 145–154. [CrossRef]
47. Gorelov, V.P.; Balakireva, V.B.; Kleshchev, Y.N.; Brusentsov, V.P. Preparation and Electrical Conductivity of $BaZr_{1-x}R_xO_{3-\alpha}$ (R = Sc, Y, Ho, Dy, Gd, In). *Inorg. Mater* **2001**, *37*, 535–538. [CrossRef]